This is a preprint of an article published in Advanced Robotics, Vol. 21, No. 1-2, pp. 23-50 (2007),
Available online http://www.ingentaconnect.com/content/vsp/arb/2007/00000021/F0020001/art00002

Stability of Autonomous Vehicle Path Tracking with Pure Delays in the Control Loop

Guillermo Heredia Anibal Ollero

Robotics, Vision and Control Group. Escuela Superior de Ingenieros, Universidad de Sevilla. Camino de los Decubrimientos s/n, 41092 - Sevilla (Spain) E-mail:guiller@cartuja.us.es,aollero@cartuja.us.es

Abstract

This paper presents a new method to analyze the stability of a general class of mobile robot path tracking algorithms taking into account explicitly the computation and communication delays in the control loop. These pure delays are present in autonomous vehicles due to position estimation. The problem is analyzed by solving directly the transcendental characteristic equation that appears when the time delay is considered. The analysis has been done for straight paths and paths of constant curvature. The method has been applied to the pure pursuit path tracking algorithm, one of the most widely used. The paper presents several tests with two different outdoor autonomous vehicles (ROMEO-3R and a computer controlled HMMWV), in spite of difficulties of practical experiments with real vehicles close to the stability limits. These tests pointed out how the predictions about the stability of the proposed methods obtained by using simple models are verified in practice with two different outdoor vehicles.

keywords: autonomous vehicles, mobile robots, path tracking, stability, time delay

1 INTRODUCTION

Path tracking is a basic function of many mobile robot or autonomous vehicle control systems. The objective of path tracking is to generate control commands for the vehicle to follow a previously defined path by taking into account the actual position and the constraints imposed by the vehicle and its lower level motion controllers.

The path can be obtained in several ways:

- Recorded by the vehicle itself when an human operator is driving. Navigation sensors (gyroscopes, compass and accelerometers) and dead reckoning are usually applied. Furthermore, Global Positioning Systems (GPS) and, particularly, Differential Global Positioning System (DGPS) are very useful to record the path in outdoor navigation [1] [2].
- Computed by a path planner-generation system [3] in a classical planned architecture for autonomous vehicle control.

- Provided in real-time by the environment perception system. This is the case when the path is defined from the perception of environment features such as lines or roads [4] [5], or when the objective is to track another vehicle or mobile object [6].

- Provided by a teleoperator from a remote station. This is an advanced teleoperation mode, also called semi-autonomous teleoperation, in which the teleoperator provides interactively segments of the path to be tracked using advanced computer interfaces [7].

Notice that, in all cases, sensing is required in real time to estimate the position and orientation of the vehicle with respect to the path to be tracked. This estimation can be performed using several sources of data including the environment perception system (image, range data, sonars) as well as internal sensors (inclinometers, gyroscopes, accelerometers) and dead reckoning techniques.

When the position and orientation estimation involves environment perception the computational delays could be important. It should be noted that delays between 0.1 and 0.5 seconds are very usual. These delays could be very significant in outdoor navigation when the velocity is high.

Furthermore, DGPS systems provide accurate position estimation but also introduces a significant delay in the loop. The magnitude of this delay depends on the required accuracy but could also be of several hundreds of milliseconds [8].

Path tracking is directly related to the lateral vehicle motion and steering control. Vehicles control also involves speed control. Obviously, both are coupled problems. However, path tracking has been usually studied for constant velocity. Thus, the path tracking algorithm implements a steering strategy (control law) by using the error between the current estimated vehicle position/orientation and the path to follow. The inputs of the path tracker are variables defining the state of the vehicle with respect to the path, and the output is the steering command to be executed by the low-level motion controllers.

The most significant dynamic effects in the vehicles control come from the vehicle-terrain interaction and from the dynamics of the actuation system. The former is hard to consider in real time due to the complex relations involved and the difficulties in sensing. However, it can be shown from experimentation that the steering actuation dynamics is relatively easy to model and has a significant impact in the path tracking performance of the vehicles [9].

On the other hand, for short intervals, the kinematic equations can be linearized for constant velocity using vehicles fixed coordinates or path dependent coordinates. Thus, the path tracking problem has been formulated for every value of the vehicle speed as a linear control problem and the dynamic of the steering actuation system can be considered as additional linear equations. Then, linear control methods has been applied for the vehicle automated steering [10] [11]. Thus, for example, Generalized Predictive Control (GPC) theory has been also applied obtaining good results [12] when the vehicle is close the path in position and heading, and there are not significant perturbations. However if, due to measuring errors or perturbations, the vehicles separates from the path, the linearization conditions are violated and the tracking deteriorates.

Several new control schemes have been proposed. Controllers based on feedback linearization [13]

and nonlinear continuous time-varying feedback controllers [14] [13] have been introduced.

Furthermore, fuzzy logic methods have been also applied with good results both for automatic tuning of other methods [15], or to generate directly the steering command by using heuristic rules [16]. This strategy leads to a nonlinear control law on the lateral error, heading and distance from the vehicle to a goal point in the path. In this case the problem pointed out is the difficulty for designing and tuning the fuzzy controller.

Many path tracking practical implementations in existing autonomous vehicles are pure pursuit strategies, because of its easy of tuning and good performance. Due to this reason, this paper considers pure pursuit as the basic technique. However, stability conditions are derived for general geometric path tracking algorithms, and can be applied to any path tracking method based on geometric considerations.

Path tracking methods have parameters related to the selection of a goal point or a particular segment of the path to follow. This point or path segment is required to compute the signal error in the path tracking loop. These parameters are related to the gain of the closed loop system and have a significant effect on the tracking performance. Thus, oscillations or even instability can arise for some values of the controller parameters. These instability conditions are related to both the vehicles characteristics and navigation conditions including speed, path to follow and terrain.

It should be noted that there are also adaptive implementations in which the parameters are tuned according to the current navigation conditions. Thus, instability can arise if the parameters are not tuned properly.

This paper investigates the dynamic behavior of path tracking. Particularly, stability conditions of the pure pursuit algorithm are studied. In the pure pursuit method, the goal-point related parameter is simply the lookahead distance from the current vehicle position to the goal point selected in the forward path to track. Then, the stability of the tracking system in terms of the lookahead is studied. The relation with the vehicles velocity is also considered in the paper.

The problem is not easy due to the nonlinear nature of the feedback tracking system. Thus, only few results have been presented in this significant problem. The stability of the controllers presented in [13] [14] is proved via Lyapunov theory.

Furthermore, notice that, as mentioned above, path tracking involves in many cases significant pure delays in the control loop due mainly to the mobile robot position estimation as well as to other computing and communication delays. The consideration of the pure delay in the path tracking loop introduces an additional complexity in the analysis. It should be noted that most stability analysis techniques can not be applied to systems with pure delays. Thus, Input-Output methods and Lyapunov techniques to analyze the stability can not be applied directly [17]. Classical frequency response methods are useful for the analysis of path tracking systems with delays [18] [19], but these methods only can be applied when the frequency response of the nonlinear part can be approximated by the describing function.

Stability analysis of path tracking loops can be performed off-line to verify a control system design or on-line to supervise the control system performance when navigation conditions change or when the

parameters of the controller are changed to adapt to different conditions (adaptive systems).

Three tools are typically used to investigate the stability of time-delay systems: Razumikhin theory, Lyapunov-Krasovskii theory and (for linear time-delay systems) eigenvalue considerations (see [20] for a good survey). However, none of these basic concepts represents applicable stability tests in terms of the system matrices. The stability of general, linear time-delay systems can be checked exactly only by eigenvalue considerations. Unfortunately, the computation of the eigenvalues is complex, since the corresponding transcendental quasi-characteristic equation contains exponential terms which induce extreme gradients, and it has an infinite number of solutions. This task can be done off-line with the help of mathematical tools widely available.

On the other hand, in situations when a solution is needed in real time, like in supervisor or adaptive systems, the direct solution of the quasi-characteristic equation is not practical. In these cases, a procedure based on [21] and [22], can be used. This technique determines the intervals of delay values for which the system is asymptotically stable for a given parameter set (the -decomposition). This procedure can be modified to obtain the stability regions in parameter space for an interval of time delays. The advantage of this method is that the transcendental characteristic quasi-polynomial is transformed into an equivalent finite polynomial, and hence posses only a finite number of solutions. Moreover, it is then possible to make use of results for delay-free systems such as the Routh-Hurwitz criterion. Using this transformation, finding the solutions of the quasi-characteristic equation is much faster, and it can be performed on-line.

This paper present a new technique to analyze path tracking control systems with pure time delays in the control loop. The technique can be applied to both conventional fixed-parameter control systems and adaptive control systems providing in this case the limits to the adaptation of the parameters. Furthermore the proposed new method can be applied to the analysis of teleoperation control systems providing limits to key parameters such as the vehicles velocity depending of the expertise of the teleoperator.

It should be noted that the practical verification of the proposed analysis methods in real vehicles is difficult, or even dangerous, due to the experiments near or over the stability limits. However, several experiments were conducted with two real outdoor vehicles to check the proposed analysis methods.

The remaining of the paper is organized as follows. Section 2 presents the formulation of the path tracking problem. The basic method for stability analysis is presented in section 3. The ability of this technique to consider systems with time delay, including simulations, is shown in section 4. Section 5 is devoted to the experiments with two different vehicles: the ROMEO 3R and the Red Zone Robotics HMMWV. Sections 6, 7 and 8 are for the Conclusions, Acknowledgments and References.

2 PATH TRACKING

Outdoors vehicle motion is a complex problem involving kinematic and dynamic motion equations, vehicle/terrain interaction, actuator dynamics, etc. But at a first approximation, a simplified 2D model

can be considered if the vehicle is assumed to move on a plane.

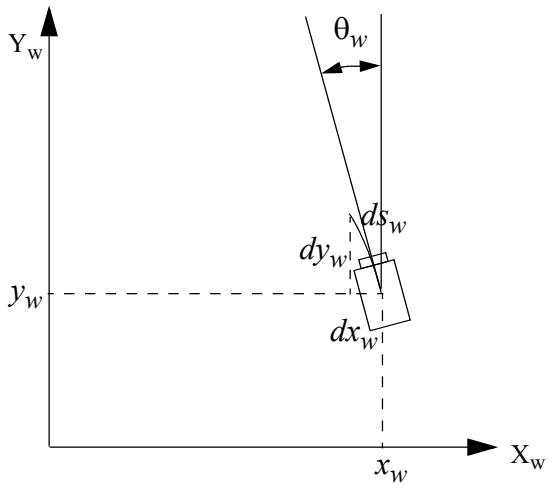

Figure 1: Vehicle kinematics.

For 2D vehicle navigation, the posture or configuration of the vehicle in world coordinates is given by (x_w, y_w, θ_w), where x_w and y_w are the vehicles coordinates, and θ_w is the orientation angle (see Figure 1). If ds_w is the distance travelled, the following expressions can be obtained:

$$dx_w = -\sin\theta_w ds_w \tag{1}$$

$$dy_w = \cos\theta_w ds_w \tag{2}$$

$$d\theta_w = \overline{\gamma} ds_w \tag{3}$$

where $\overline{\gamma}$ is the vehicle curvature, and the subscript w stands for the world coordinates (see Figure 1). Thus, the motion equations in world coordinates can be expressed as:

$$\dot{x}_w = -V\sin\theta_w \tag{4}$$

$$\dot{y}_w = V\cos\theta_w \tag{5}$$

$$\dot{\theta}_w = V\overline{\gamma} \tag{6}$$

where V is the longitudinal velocity or vehicle speed. It has been shown that the dynamics of the steering actuation system can be represented by means of first or second order linear dynamical models. In this paper the following first order model will be used:

$$\dot{\overline{\gamma}} = -\frac{1}{T}(\overline{\gamma} - \overline{\gamma_R}) \tag{7}$$

where the requested vehicles curvature γ_R is the control variable computed by the steering control algorithm, and T is the time constant.

Thus, the steering control system can be represented by means of equations (4), (5), (6) and (7), where x_w, y_w, θ_w and $\overline{\gamma}$ are the state variables.

Several path tracking algorithms select a goal point on the path at a fixed distance from the vehicle that is called the lookahead distance $\overline{L}$, as shown in Figure 2. Using this goal point three values are obtained that are the inputs to the path tracker. These inputs are the lateral position error in vehicle coordinates x_l, the orientation error with respect to the goal point θ_w^e and the curvature error with respect to the goal point γ^e. The expressions of θ_w^e and γ^e are:

$$\begin{aligned} \theta_w^e &= \theta_w - \theta_w^{path} \\ \gamma^e &= \overline{\gamma} - \gamma^{path} \end{aligned} \tag{8}$$

where θ_w^{path} and γ^{path} are the orientation and curvature of the path at the goal point.

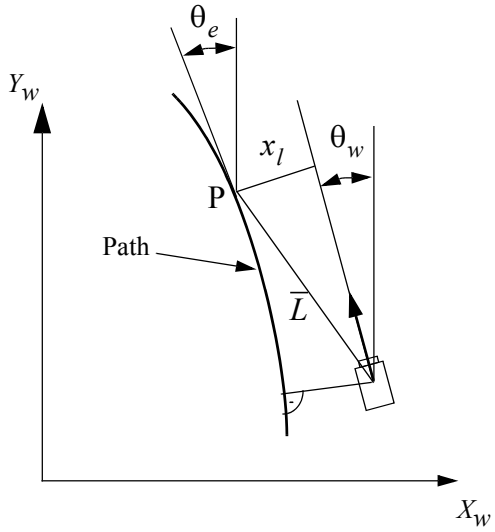

Figure 2: Path Tracking.

The objective of path tracking is that the vehicle follows a given path. As mentioned above, path tracking algorithms involve the obtaining of a goal point in the path at a fixed lookahead distance $\overline{L}$, and the computation of the lateral distance x_l in local coordinates.

For straight paths and circular paths, explicit expressions of x_l as a function of $\overline{L}$ can be obtained. However, for an arbitrary path, there is no closed-form expression for x_l. Obtaining the goal point involves solving an optimization problem in the general case.

It can be noted that in [23] it has been argued that any path can be suitably broken down into straight line and circular arc segments. In fact, the paths used in many practical applications can be approximated by connected straight line and circular arc segments. In this paper the stability of the path tracking problem is studied for these two basic paths (straight and circular).

2.1 Tracking of straight paths.

Consider a straight line as a path to follow, and a reference system $X_S - Y_S$ with the axis in the same direction than the path (see Figure 3). Then, in this system $\theta_w^{path} = 0$ and $\gamma^{path} = 0$ at all the points

of the path.

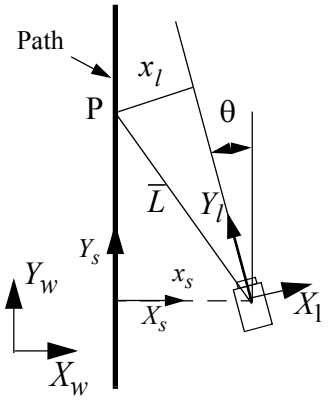

Figure 3: Straight path tracking.

Therefore,

$$\begin{aligned} \theta_w^e &= \theta_s \\ \gamma^e &= \overline{\gamma} \end{aligned} \tag{9}$$

where θ_s is the orientation of the vehicle with respect to the path and the expression of the lateral position error can be obtained from Figure 3:

$$x_l = -(x_s \cos\theta_s - \sqrt{\overline{L}^2 - x_s^2}\ \sin\theta_s) \tag{10}$$

It can be observed that for straight path tracking the expressions of the path tracking algorithm inputs θ_w^e, γ^e and x_l do not depend on the y_l variable, and therefore equation (5) can be omitted. Thus, the system model is the following:

$$\begin{aligned} \dot{x}_s(t) &= -V \sin\theta_s(t) \\ \dot{\theta}_s(t) &= V\overline{\gamma}(t) \\ \dot{\overline{\gamma}}(t) &= -\frac{1}{T}(\overline{\gamma}(t) - \overline{\gamma_R}(t-\overline{\tau})) \end{aligned} \tag{11}$$

where $\overline{\tau}$ is the pure time delay in the control loop.

2.1.1 Non-dimensional equations

In order to simplify the equations and decrease the number of parameters in the model, consider the following non-dimensional variables:

$$x = \frac{x_s}{VT}\ ,\ \theta = \theta_s\ ,\ \gamma = VT\overline{\gamma}\ ,\ \tau = \frac{\overline{\tau}}{T} \tag{12}$$

The equations of the model are now:

$$\dot{x}(t) = \sin\theta(t)$$

$$\begin{aligned} \dot{\theta}(t) &= \gamma(t) \\ \dot{\gamma}(t) &= -\gamma(t) + \gamma_R(t-\tau)) \end{aligned} \tag{13}$$

where γ_R is the non-dimensional form of the control law. t is now the non-dimensional time related with t in former expressions according to t/T.

2.2 Constant curvature path tracking

Consider now the tracking of a constant curvature path. The goal of this analysis is the stability of the path tracking system. Therefore, when tracking circular paths it is more convenient to express the equations in polar coordinates. In this way, the equilibrium state of the system (the vehicle following perfectly the path) is the origin of the system.

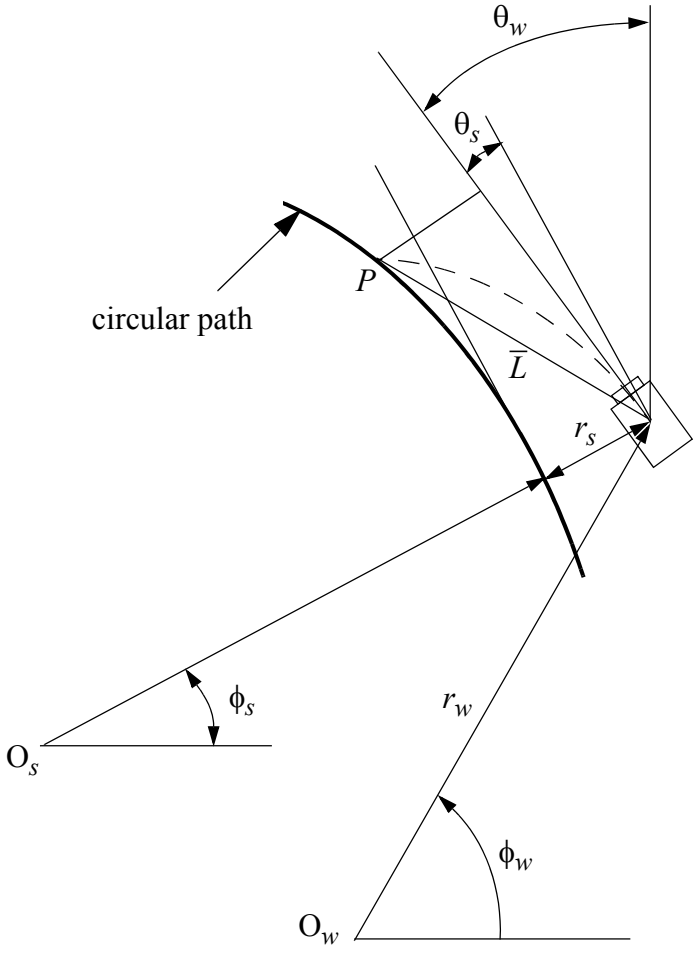

Figure 4: Pure pursuit circular path tracking.

2.2.1 Equations in polar coordinates

In polar world coordinates, the position of the vehicle is expressed as the distance r_w and angle ϕ_w from the origin O_w (see Figure 4). The orientation of the vehicle is θ_w. As the objective of the analysis is the stability of the motion of the vehicle tracking the circular path of Figure 4, a new coordinate system with origin O_s (the center of the circular path) will be used. The variables are defined as follows: r_s is the radial distance from the path to the vehicle, θ_s is the angle between the vehicle heading and the normal to the radius, and the curvature $\overline{\gamma}$ is defined as:

$$\overline{\gamma} = \gamma_w - \overline{\gamma}^{path} \tag{14}$$

where γ_w is the absolute curvature, and $\overline{\gamma}^{path} = 1/R$ is the constant path curvature, where R is the curvature radius. In this coordinate system, the equations of motion are:

$$\begin{aligned} \dot{r}_s &= -V \sin\theta_s \\ \dot{\theta}_s &= V\left(\overline{\gamma} + \overline{\gamma}^{path} - \frac{\overline{\gamma}^{path}\cos\theta_s}{1 + r_s\overline{\gamma}^{path}}\right) \\ \dot{\overline{\gamma}} &= -\frac{\overline{\gamma} + \overline{\gamma}^{path}}{T} + \frac{\overline{\gamma}_R}{T} \end{aligned} \tag{15}$$

It can be noted that using this reference system, the origin of the system ($r_s = 0$, $\theta_s = 0$, $\overline{\gamma} = 0$) represents a situation in which the vehicle is following perfectly the circular path and, therefore, the objective of the path tracking algorithm is to drive the system to the origin. If the system is expressed using non-dimensional variables, the equations are:

$$\begin{aligned} \dot{r} &= -\sin\theta \\ \dot{\theta} &= \gamma + \gamma_p - \frac{\gamma_p\cos\theta}{1 + r\gamma_p} \\ \dot{\gamma} &= -(\gamma + \gamma_p) + \gamma_R \end{aligned} \tag{16}$$

where the following non-dimensional variables have been used:

$$r = \frac{r_s}{VT} \;\;,\;\; \theta = \theta_s \;\;,\;\; \gamma = VT\overline{\gamma} \;\;,\;\; \gamma_p = VT\gamma^{path} \;\;,\;\; \gamma_R = VT\overline{\gamma}_R \tag{17}$$

2.3 Pure pursuit path tracking

The pure pursuit strategy [24] is based on very simple geometric considerations. The path is tracked by repeatedly fitting circular arcs to different goal points on the path as the vehicle moves forward. Let $\overline{L}$ be the lookahead (distance from the vehicle to an objective point in the path) and (x_l,y_l) be the coordinates of the objective point P in a local frame attached to the vehicle. Figure 5 illustrates how the arc fitting is performed. From this figure the following equations holds:

$$(r - x_l)^2 + y_l^2 = r^2 \tag{18}$$

where r is the radius of the circular arc. Solving this equation for r the following expression is obtained:

$$r = \frac{x_l^2 + y_l^2}{2x_l} \tag{19}$$

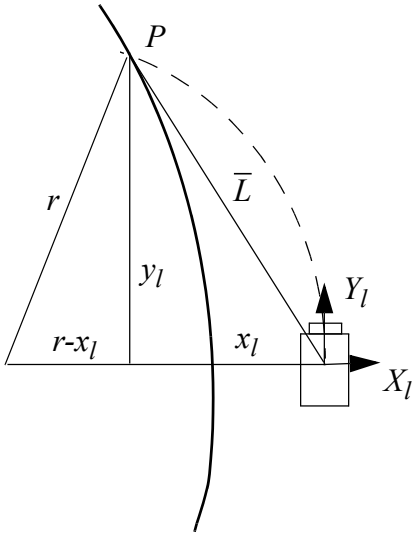

Figure 5: Pure pursuit arc fitting.

Thus, the steering command is the requested new curvature ($\gamma_R = 1/r$) which can be computed by:

$$\gamma_R = \frac{-2x_l}{\overline{L}^2} \tag{20}$$

where x_l is the x-displacement of the goal point in vehicle coordinates (lateral displacement) and $\overline{L}$ is the lookahead distance. Thus, the pure pursuit method is a proportional controller of the steering angle using the lookahead for the gain and the local coordinate x_l as the error. It is necessary to choose a good goal point in the map according with the current navigation conditions. In fact, if the goal point is too far, the vehicle may cut corners and if too near, oscillations may result. As it will seen in the next section, there is a minimum value of $\overline{L}$ to maintain the stability of the system. Observe how for $\overline{L} \to \infty$ in (20) the controller gain tends to zero and no steering corrections at all are introduced. However, for short lookaheads the gains is high.

In what follows, the non-dimensional form of the lookahead will be used:

$$L = \frac{\overline{L}}{VT} \tag{21}$$

To conclude this section note that the conventional pure pursuit strategy does not consider the vehicles dynamics; however from experimentation it can be shown that the steering dynamics (7) has a significant influence on the behavior of the vehicle. Thus, this dynamics will be considered in the following sections.

3 Non-delayed stability analysis

Regarding the stability issue, two different problems can be stated: a local one, the stability around the operating point; and a global one, the appearance of equilibria different from the origin. The analysis

will be done separately for straight line and circular paths.

3.1 Straight line paths.

3.1.1 Equilibrium points.

Consider first the existence of equilibrium points different from the origin. The equilibrium points of system (13) are the values of x, θ and γ that are solutions to:

$$\begin{aligned} -\sin\theta &= 0 \\ \gamma &= 0 \\ -\gamma + \gamma_R(x,\theta,\gamma) &= 0 \end{aligned} \tag{22}$$

If $\gamma_R(x,\theta,\gamma) = 0$, then the point $(0,0,0)$ is a solution of (23). There exist other solutions for $\theta = \pm l\pi$, being l an integer. However, only the equilibria for $l = 1$ will be considered in the sequel. The existence of equilibrium points other than the origin will depend on the expression of the steering command $\gamma_R(x,\theta,\gamma)$.

3.1.2 Local stability analysis.

Consider now the stability around the operating point. Local stability of an equilibrium state of a nonlinear system may be examined by stability of the linearized system around the equilibrium state. This analysis applies only in the neighborhood of the equilibrium state. In the path tracking problem, the vehicle is trying to follow the path, so the vehicles state will be in the vicinity of the equilibrium state, and therefore the above assumption is acceptable.

Stability analysis for delay-free linear systems is well established, and algebraic stability conditions can be obtained as a function of the parameters. Consider the following linear autonomous system:

$$\dot{x}(t) = A_0 x(t) \tag{23}$$

where $x \in \mathbb{R}^n$ and $A_0 \in \mathbb{R}^{n\times n}$. In the following, $Re(s)$ designates the real part of s, and $\mathbb{C}$ is the set of complex numbers. The so-called characteristic equation for the linear differential equation (23) is given by:

$$det[\Delta(s)] = det[sI - A_0] \tag{24}$$

The necessary and sufficient condition for delay-free linear systems to be uniformly asymptotically stable is that $Re(s) < 0$ for all $s \in \mathbb{C}$ satisfying $det[\Delta(s)] = 0$, i.e. that all the roots of the characteristic equation have negative real part. This condition can be assured by the well-known Routh-Hurwitz criterion.

Consider the motion equations of the non-delayed path tracking problem in non-dimensional form

(13) with $\tau = 0$. The linearized system around the origin is:

$$\begin{bmatrix} \dot{x} \\ \dot{\theta} \\ \dot{\gamma} \end{bmatrix} = J \begin{bmatrix} x \\ \theta \\ \gamma \end{bmatrix} \tag{25}$$

where J is the Jacobian of the nonlinear system:

$$J = \begin{bmatrix} 0 & -1 & 0 \\ 0 & 0 & 1 \\ \varphi_x & \varphi_\theta & (\varphi_\gamma - 1) \end{bmatrix} \tag{26}$$

where $\varphi_x = \frac{\partial \gamma_R}{\partial x}\Big|_0$, $\varphi_x = \frac{\partial \gamma_R}{\partial \theta}\Big|_0$ and $\varphi_x = \frac{\partial \gamma_R}{\partial \gamma}\Big|_0$ are the partial derivatives of γ_R at the origin. Let $P(s)$ be the characteristic polynomial of the linearized system:

$$P(s) = |sI - J| = s^3 + s^2(1 - \varphi_\gamma) - s\varphi_\theta + \varphi_x \tag{27}$$

Using the Routh-Hurwitz criterion, the following stability conditions can be obtained:

$$\begin{aligned} 1 - \varphi_\gamma &> 0 \\ \varphi_x &> 0 \\ -\varphi_\theta(1 - \varphi_\gamma) - \varphi_x &> 0 \end{aligned} \tag{28}$$

3.1.3 Pure pursuit straight-line tracking.

Consider the tracking of a straight line as shown in Figure 3. In this case, x_l is given by (10). By substituting in (20) and using the non-dimensional variables, the resulting steering command is:

$$\gamma_R = \frac{2}{L^2}\left[x\cos\theta - \sqrt{L^2 - x^2}\,\sin\theta\right] \tag{29}$$

The existence of equilibrium points other than the origin can be obtained from the solution to the following system of equations:

$$\begin{aligned} -\sin\theta &= 0 \\ \gamma &= 0 \\ -\gamma + \frac{2}{L^2}\left[x\cos\theta - \sqrt{L^2 - x^2}\,\sin\theta\right] &= 0 \end{aligned} \tag{30}$$

System (30) has two solutions: $(0, 0, 0)$ and $(0, \pi, 0)$. The first is the operating point (the vehicle tracking perfectly the path) and the second one corresponds to the vehicle heading in the opposite direction. Thus, it is acceptable that the trajectories will not go out of the attraction basin of the operating point in normal path tracking operation. In other words, with the perturbations found in practice, the trajectories will remain in the attraction basin of the operating point, and therefore the local stability analysis holds.

Consider now the local stability analysis of the pure pursuit path tracking. The partial derivatives $\varphi_x, \varphi_\theta, \varphi_\gamma$ are:

$$\varphi_x = \frac{2}{L^2} \ , \ \varphi_\theta = \frac{-2}{L} \ , \ \varphi_\gamma = 0 \tag{31}$$

The two first conditions of Equations (27) are always true, and the third one becomes:

$$L > 1 \tag{32}$$

Thus, the non-delayed pure pursuit algorithm will be stable if condition (32) holds.

3.2 Circular paths.

3.2.1 Equilibrium points.

Consider first the existence of equilibrium points different from the origin. The equilibrium points of system (16) are the values of r, θ and γ that are solutions to:

$$\begin{aligned} \sin\theta &= 0 \\ \gamma + \gamma_p - \frac{\gamma_p \cos\theta}{1 + r\gamma_p} &= 0 \\ -(\gamma + \gamma_p) + \gamma_R(r, \theta, \gamma) &= 0 \end{aligned} \tag{33}$$

If $\gamma_R(0,0,0) = 0$, then the point $(0,0,0)$ is a solution of (33). The existence of other equilibrium points other than the origin will depend on the expression of the steering command $\gamma_R(r, \theta, \gamma)$.

3.2.2 Local stability analysis.

The local stability of the nonlinear system (33) can be studied linearizing the system around the equilibrium point. In this case, the Jacobian matrix J is:

$$J = \begin{bmatrix} 0 & -1 & 0 \\ \gamma_p^2 & 0 & 1 \\ \varphi_r & \varphi_\theta & (\varphi_\gamma - 1) \end{bmatrix} \tag{34}$$

The characteristic polynomial is:

$$Q(s) = s^3 + s^2(1 - \varphi_\gamma) + s(\gamma_p^2 - \varphi_\theta) + (\varphi_r + \gamma_p^2(1 - \varphi_\gamma)) \tag{35}$$

In the same way than for straight paths, the following stability conditions can be obtained using the Routh-Hurwitz criterion:

$$\begin{aligned} 1 - \varphi_\gamma &> 0 \\ \gamma_p^2 - \varphi_\theta &> 0 \\ \varphi_r + \gamma_p^2(1 - \varphi_\gamma) &> 0 \\ -\varphi_\theta(1 - \varphi_\gamma) - \varphi_r &> 0 \end{aligned} \tag{36}$$

3.2.3 Pure pursuit circular path tracking.

Consider the tracking of the constant curvature path shown in Figure 4. For pure pursuit path tracking, γ_R is:

$$\gamma_R = \frac{2}{L}\left[\frac{\gamma_p(r^2+L^2)+2r}{2L(1+\gamma_p r)}\cos\theta - \sqrt{1-\left(\frac{\gamma_p(r^2+L^2)+2r}{2L(1+\gamma_p r)}\right)^2}\sin\theta\right] \tag{37}$$

and

$$\begin{aligned} \varphi_r &= \frac{2}{L^2}\left(1-\frac{\gamma_p^2 L^2}{2}\right) \\ \varphi_\theta &= -\frac{2}{L}\sqrt{1-\frac{\gamma_p^2 L^2}{4}} \\ \varphi_\gamma &= 0 \end{aligned} \tag{38}$$

Substituting the values (38) in the conditions (36), it can be seen the first three conditions are always fulfilled, and the last one leads to the following inequality:

$$\frac{2}{L}\sqrt{1-\frac{\gamma_p^2 L^2}{4}} - \frac{2}{L^2}\left(1-\frac{\gamma_p^2 L^2}{2}\right) > 0 \tag{39}$$

This inequality can be solved for L as a function of γ_p, resulting in:

$$L > \sqrt{\frac{2}{1+\gamma_p^2} + \frac{2}{\gamma_p^2(1+\gamma_p^2)} - \frac{2}{\gamma_p^2\sqrt{1+\gamma_p^2}}} \tag{40}$$

In Figure 6 the limit value of L is plotted as a function of γ_p. It can be seen that, for usual values of γ_p (the values plotted in Figure 6), this limit L is close to 1.

Therefore, the tracking of constant curvature paths will be stable if L fulfills condition (40), this is, if the value of L is in the stable region of Figure 6.

4 Stability of path tracking with time delays.

Consider now the following delay-differential system:

$$\dot{x}(t) = A_0 x(t) + A_1 x(t-\tau) \tag{41}$$

where $x \in \mathbb{R}^n$, $A_0, A_1 \in \mathbb{R}^{n\times n}$ and $\tau \in [0,\infty)$ is the time delay present in the feedback loop. The so-called characteristic quasi-polynomial for the linear differential equation (41) is given by:

$$det[\Delta(s)] = det[sI - A_0 - A_1 e^{-s\tau}] \tag{42}$$

The necessary and sufficient condition for delay-differential linear systems to be uniformly asymptotically stable is that $Re(s) < 0$ for all $s \in \mathbb{C}$ satisfying $det[\Delta(s)] = 0$ (see, for example, [25]). In this case, the stability conditions cannot be established in terms of the system coefficients. In the general case, the transcendental equation (which has an infinite number of roots) has to be solved.

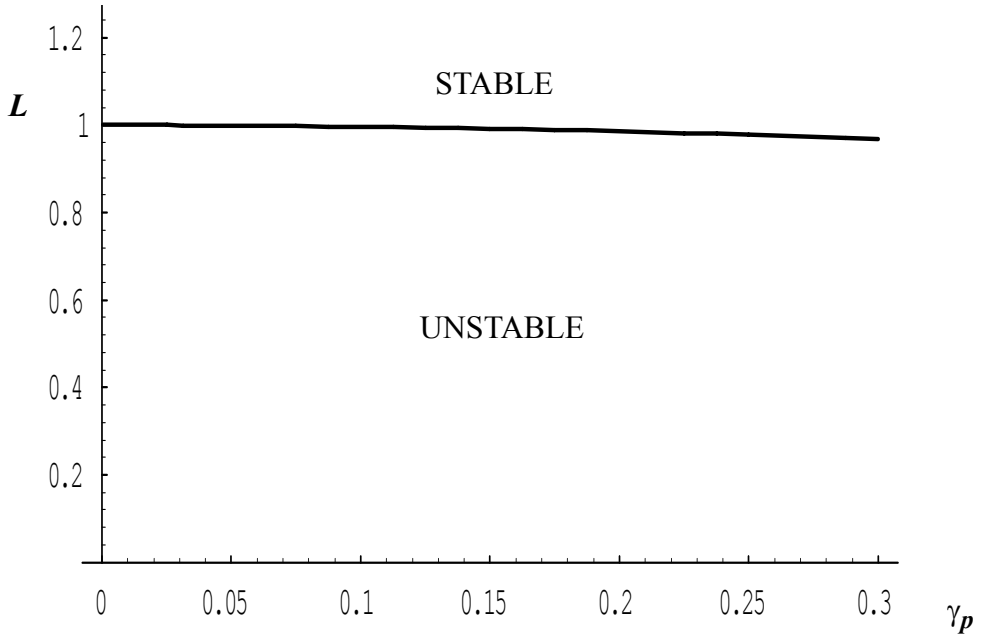

Figure 6: Limit L as a function of γ_p for circular paths.

4.1 Straight paths.

Consider now the problem of path tracking with time delays. The equilibrium points of system (13) are the values of x, θ and γ that are solutions to:

$$\begin{aligned} \sin\theta(t) &= 0 \\ \gamma(t) &= 0 \\ -\gamma(t) + \gamma_R(x(t-\tau), \theta(t-\tau), \gamma(t-\tau)) &= 0 \end{aligned} \tag{43}$$

If $\gamma_R(0,0,0) = 0$, then the point $(0,0,0)$ is a solution of (43). The existence of other equilibrium points other than the origin will depend on the expression of the steering command.

Consider now the local stability analysis with time delays. The linearization of the system around the operating point takes now the following expression:

$$\begin{bmatrix} \dot{x}(t) \\ \dot{\theta}(t) \\ \dot{\gamma}(t) \end{bmatrix} = J \begin{bmatrix} x(t) \\ \theta(t) \\ \gamma(t) \end{bmatrix} + J_\tau \begin{bmatrix} x(t-\tau) \\ \theta(t-\tau) \\ \gamma(t-\tau) \end{bmatrix} \tag{44}$$

where J is the Jacobian matrix and J_τ is the Jacobian with respect to the delayed variables:

$$J = \begin{bmatrix} 0 & -1 & 0 \\ 0 & 0 & 1 \\ 0 & 0 & -1 \end{bmatrix} \qquad J_\tau = \begin{bmatrix} 0 & 0 & 0 \\ 0 & 0 & 0 \\ \varphi_x & \varphi_\theta & \varphi_\gamma \end{bmatrix} \tag{45}$$

Let $Q(s)$ be the characteristic quasi-polynomial of the linearized system. $Q(s)$ is defined as:

$$Q(s) = det[sI - J - J_\tau e^{-s\tau}] \tag{46}$$

For system (44), $Q(s)$ is:

$$Q(s) = s^3 + s^2 + (-s^2\varphi_\gamma - s\varphi_\theta + \varphi_x)e^{-s\tau} \tag{47}$$

As mentioned in the above section, the roots of the characteristic quasi-polynomial have to be found. Provided that $e^{-j\omega\tau} = \cos(\tau\omega) - j\sin(\tau\omega)$, the following two conditions for the real and imaginary parts can be obtained:

$$-\omega^2 + (\omega^2\varphi_\gamma + \varphi_x)\cos(\tau\omega) - \omega\varphi_\theta \sin(\tau\omega) = 0 \tag{48}$$

$$-\omega^3 - \omega\varphi_\theta \cos(\tau\omega) - (\omega^2\varphi_\gamma + \varphi_x)\sin(\tau\omega) = 0 \tag{49}$$

The solutions to this pair of transcendental equations give the roots of the characteristic quasi-polynomial. Note that the eigenvalues can also be calculated using the τ-decomposition method [21] [22].

4.1.1 Pure pursuit tracking of straight-line paths with time delays.

If the time delay in the control loop is considered, the equilibrium points of the system are the same: $(0, 0, 0)$, $(0, \pi, 0)$ and therefore, the local stability analysis around the origin is sufficient for normal operation.

For the pure pursuit control strategy, φ_x, φ_θ and φ_γ are defined by (31). Then, the two stability equations are:

$$-\omega^2 + \frac{2}{L^2}\cos(\tau\omega) + \frac{2}{L}\omega\sin(\tau\omega) = 0 \tag{50}$$

$$-\omega^3 + \frac{2}{L}\omega\cos(\tau\omega) - \frac{2}{L^2}\sin(\tau\omega) = 0 \tag{51}$$

Using τ as a parameter, the stable limit value of the non-dimensional lookahead L can be obtained solving the nonlinear system of equations (49). Figure 7 shows the limits as a function of the non-dimensional delay τ.

4.1.2 Simulation results.

The results of Figure 7 have been confirmed with simulations of the full system with different values of L an the time delay τ. As an example, in Figure 8 the time evolution of the $x(t)$ variable is plotted for different values of L (3, 1.8 and 0.9) and the time delay τ (0, 0.55 and 1.2). These two last values of the time delay are the ones that are present in the HMMWV and ROMEO-3R autonomous vehicles with which the experiments described in section 5 have been performed.

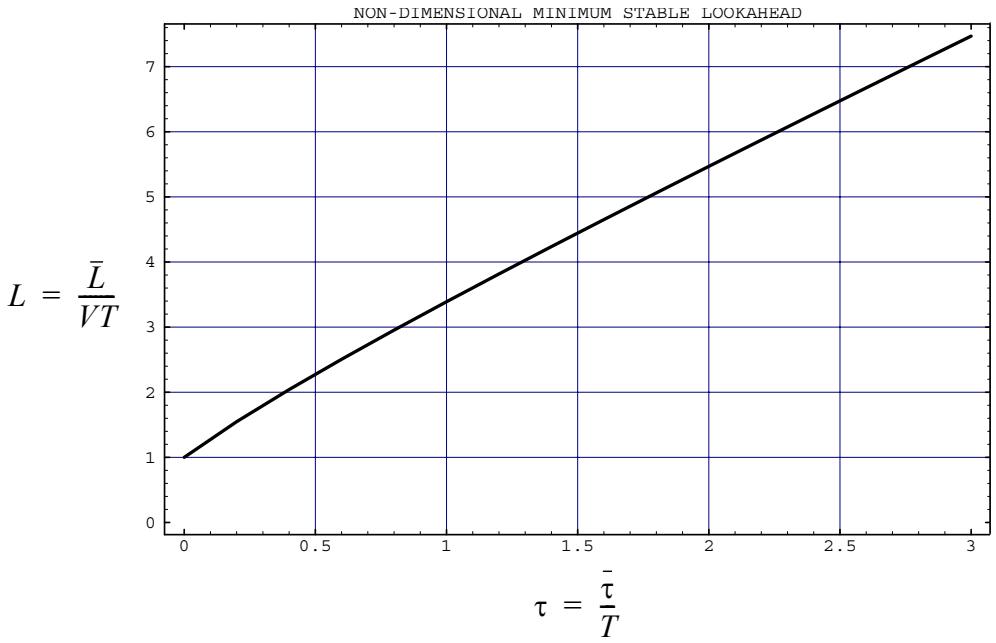

Figure 7: Straight path stable lookahead limits.

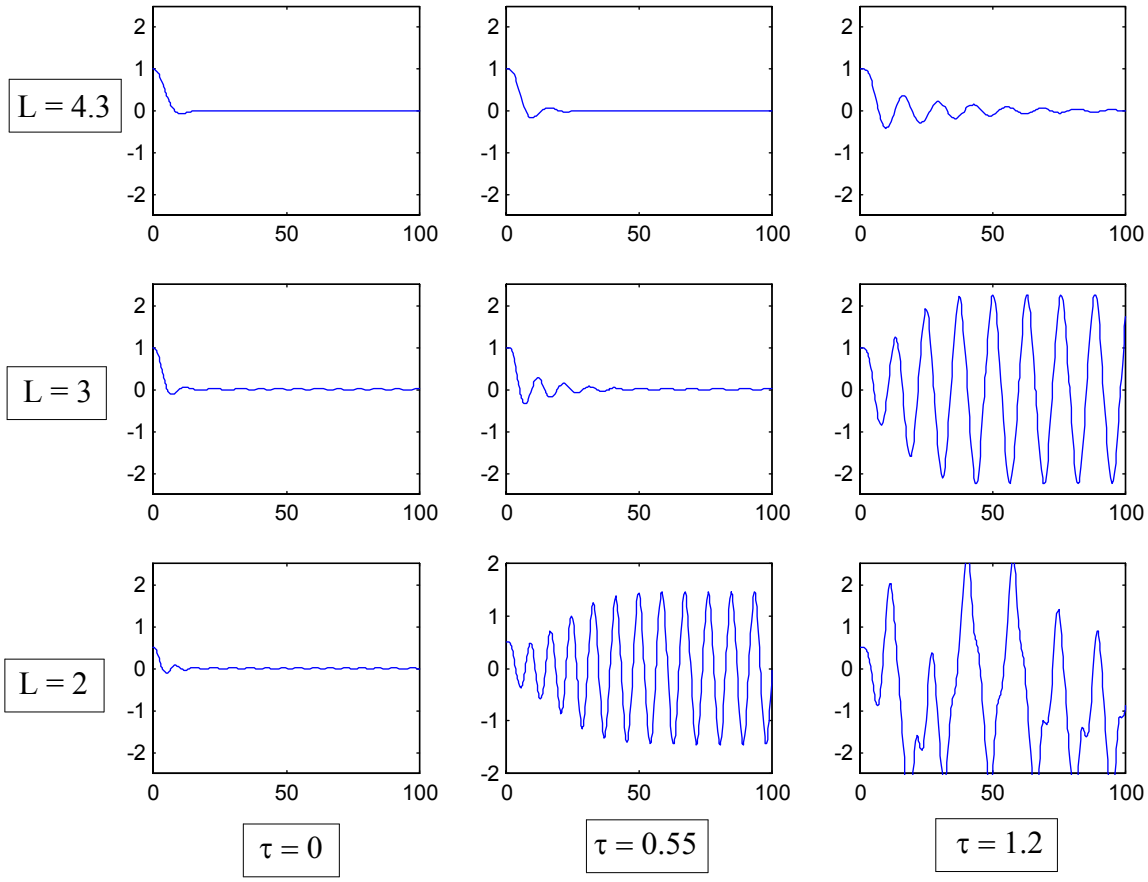

Figure 8: Time evolution of the $x(t)$ variable for different values of L and τ.

4.2 Circular paths.

Consider first the existence of equilibrium points different from the origin. The equilibrium points of system (16) are the values of r, θ and γ that are solutions to:

$$\begin{aligned} \sin\theta &= 0 \\ \gamma + \gamma_p - \frac{\gamma_p \cos\theta}{1 + r\gamma_p} &= 0 \\ -(\gamma + \gamma_p) + \gamma_R(r, \theta, \gamma) &= 0 \end{aligned} \tag{52}$$

If $\gamma_R(0,0,0) = 0$, then the point $(0,0,0)$ is a solution of Equation (50), as was the case with the non-delayed analysis. The existence of other equilibrium points other than the origin will depend on the expression of the steering command $\gamma_R(r, \theta, \gamma)$.

4.2.1 Local stability analysis.

The local stability of the nonlinear system (16) can be studied linearizing the system around the equilibrium point. In this case, the Jacobians J and J_τ are:

$$J = \begin{bmatrix} 0 & -1 & 0 \\ \gamma_p^2 & 0 & 1 \\ 0 & 0 & -1 \end{bmatrix} \qquad J_\tau = \begin{bmatrix} 0 & 0 & 0 \\ 0 & 0 & 0 \\ \varphi_r & \varphi_\theta & \varphi_\gamma \end{bmatrix} \tag{53}$$

The characteristic quasi-polynomial is:

$$Q(s) = s^3 + s^2 + \gamma_p^2 s + \gamma_p^2 + [-s^2\varphi_\gamma - s\varphi_\theta + (\varphi_r - \gamma_p^2\varphi_\gamma)]e^{-s\tau} \tag{54}$$

The roots of the characteristic quasi-polynomial $Q(s)$ can be obtained solving the equation $Q(j\omega) = 0$. The following two equations result if the real and imaginary parts are separated:

$$-\omega^2 + (\omega\varphi_\gamma + \varphi_r - \gamma_p^2\varphi_\gamma)\cos(\tau\omega) - \omega\varphi_\theta \sin(\tau\omega) + \gamma_p^2 = 0 \tag{55}$$

$$-\omega^3 + \gamma_p^2\omega - \omega\varphi_\theta\cos(\tau\omega) + (-\omega^2\varphi_\gamma - \varphi_r + \gamma_p^2\varphi_\gamma)\sin(\tau\omega) = 0 \tag{56}$$

The solutions to these simultaneous equations define the stability limits of the system. The solution can also be obtained in this case with the τ-decomposition method.

4.2.2 Pure pursuit tracking of circular paths with time delays.

Substituting (38) in (53), the stability conditions are:

$$-\omega^2 + \frac{2}{L^2}\left(1 - \frac{\gamma_p^2 L^2}{2}\right)\cos(\tau\omega) + \frac{2}{L}\sqrt{1 - \frac{\gamma_p^2 L^2}{4}}\omega\sin(\tau\omega) + \gamma_p^2 = 0 \tag{57}$$

$$-\omega^3 + \gamma_p^2\omega + \frac{2}{L}\sqrt{1 - \frac{\gamma_p^2 L^2}{4}}\omega\cos(\tau\omega) - \frac{2}{L^2}\left(1 - \frac{\gamma_p^2 L^2}{2}\right)\sin(\tau\omega) = 0 \tag{58}$$

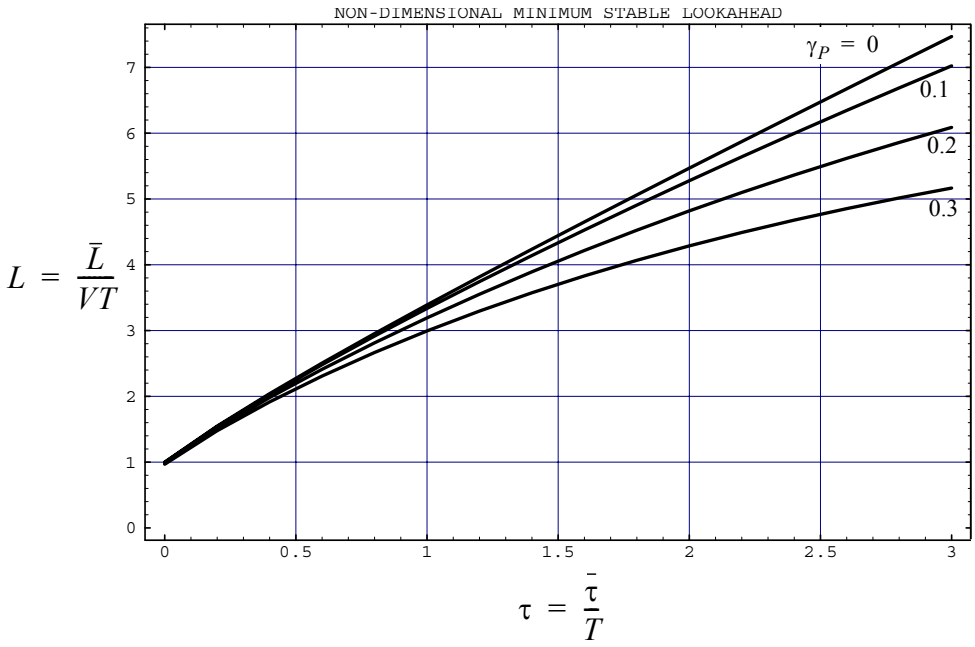

Figure 9: Circular path stable lookahead limits.

The stable limit values of the non-dimensional lookahead L are shown in Figure 9 for several path curvatures.

The results presented in this section have been also checked with simulations.

5 Experimental results.

5.1 Description of the tests in autonomous navigation.

Several tests have been made to check the theoretical results explained in the preceding sections, using the pure pursuit path tracking algorithm. These tests have been made with the ROMEO-3R and HMMWV autonomous vehicles for different values of the forward velocity. ROMEO-3R (see Figure 10a) is an outdoor robotic three-wheeled vehicle developed by the Robotics, Vision and Control Group of the University of Seville (Spain), that can be used as a testbed for mobile robotics and autonomous vehicle control [26]. The computer controlled HMMWV (see Figure 10b) from RedZone Robotics, Inc. (Pittsburgh, PA, USA) has been modified so that it can be driven automatically. Early preliminary results have been presented in [27].

Figure 10: a) ROMEO-3R b) HMMWV from RedZone Robotics.

In each test performed with the HMMWV, the vehicle was commanded to follow a path, starting at a point slightly separated from the path. The tests were carried out in a 500 m. long and 10 m.

width road. This road is almost straight, with a curved section of small curvature. Therefore, the theoretical limits for $\gamma_p = 0$ have been used. The estimated time delay for the test vehicle is $\tau = 0.55$ s. This includes computing, communication and actuator delays. The time constant of the steering system is estimated to be $T = 1.3$ s. Notice that the delay is very significant when comparing with this time-constant.

The purpose of these experiments is the determination of the stability limit, i.e. the value of the parameter $L = \overline{L}/VT$ for which the behavior of the vehicle changes from stable to unstable. In practice, it is impossible to obtain a single value of the parameter. In turn, the following procedure was adopted:

1. Choose a value of L for which the motion is stable. Make experiments with decreasing values of L that maintain stability. Record the smallest L for stable motion.

2. Choose a value of L for which the motion is unstable. Make experiments with increasing values of L that makes the motion unstable. Record the largest L for unstable motion.

The stability limit should be between these two experimental values obtained in steps 1 and 2.

To illustrate the experiments that were performed with the HMMWV autonomous vehicle, the trajectories followed by the vehicle with two different controllers are presented in Figures 11 and 12. In Figure 11 the controller is using a lookahead distance that made the motion unstable. Therefore, small deviations from the path were amplified quickly, and the supervisor had to take control of the vehicle to avoid hitting obstacles on the sides of the road. In Figure 12, the controller uses a lookahead distance that made the motion stable. In this case, the vehicle was able to follow the road, but with considerable oscillation around it. This is due to the fact that lookaheads only slightly higher than the ones that made the trajectories unstable were used. It is important to note that these experiments were designed specially to check the stability results developed in this paper. Using a larger lookahead distance the vehicle was able to track the road without oscillations (this experiments are not presented here).

Several runs were performed for three vehicle velocities (3, 6 and 9 m/s). In each test, the minimum lookahead L that made the motion stable and the maximum L that made the motion unstable were recorded.

In the ROMEO 3R vehicle, the time constant of the steering system and the delay in the control loop were estimated to be $T = 0.25$ s. and $\tau = 0.3$ s. respectively. The tests with ROMEO 3R were done with velocities of 0.4, 0.8 and 1.2 m/s. Experiments were done with straight paths and with curved paths of different curvatures.

The procedure was the same than in the experiments with the HMMWV described above. For each velocity, the minimum lookahead L that made the motion stable and the maximum L that made the motion unstable were recorded.

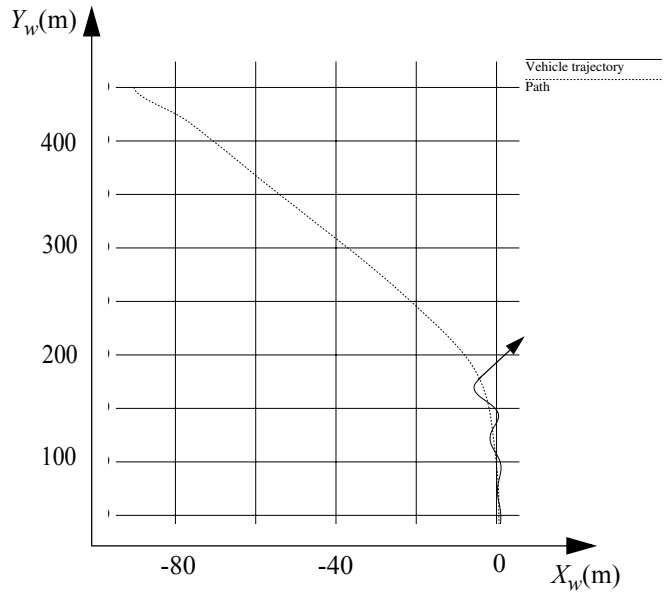

Figure 11: Unstable trajectory.

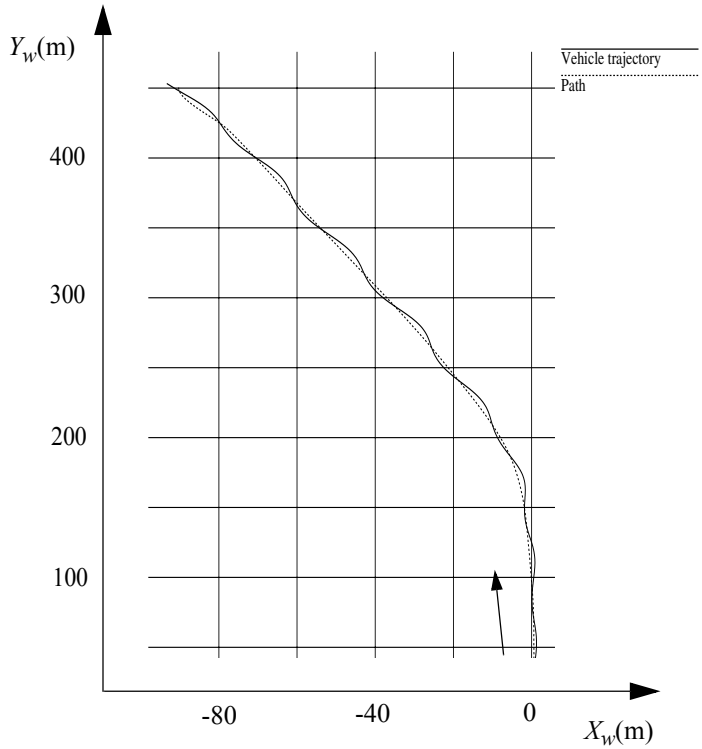

Figure 12: Stable trajectory.

5.2 Straight path experiments.

5.2.1 HMMWV tests.

As was mentioned in the last section, the tests with the HMMWV vehicle were done on an almost straight road, and therefore the results are compared to the theoretical stability limits for straight paths (see Figure 13). The non-dimensional time delay for the HMMWV vehicle is $\tau 1 = 0.55$ s.

Several experiments were done with the HMMWV vehicle at different velocities (3, 6 and 9 m/s), as was explained in section 5.1. The minimum lookahead that made the motion stable (L_{stable}), and the maximum L that made the motion unstable ($L_{unstable}$) obtained in the experiments are shown in Table 1.

Table 1: HMMWV vehicle experimental results

	$V = 3$ m/s	$V = 6$ m/s	$V = 9$ m/s
L_{stable}	2.70	2.60	2.60
$L_{unstable}$	2.15	2.10	2.15

In Figure 13 these values are shown superimposed with the theoretical results obtained in the preceding sections. For clarity, only one of the values is plotted (the worst case): L_{stable} is represented with a cross, and $L_{unstable}$ with a square. The stability limit corresponding to the time delay τ_1 should be between the cross and the square. The theoretical limit value if the time delay is not considered ($L = 1$) is represented with a solid horizontal line. It can be seen that the results predicted with no time delay are very different from the experimental results, while the results predicted considering the time delay agree with the experiments.

5.2.2 ROMEO-3R tests.

The test with the ROMEO-3R vehicle were done on an straight path at different velocities (0.4, 0.8 and 1.2 m/s). The non-dimensional time delay for the ROMEO-3R vehicle is $\tau_2 = 1.2$ s. As was done with the HMMWV experiments, the minimum lookahead that made the motion stable (L_{stable}), and the maximum L that made the motion unstable ($L_{unstable}$) obtained in the experiments were recorded. The results are presented in Table 2.

Table 2: ROMEO-3R experimental results

	$V = 0.4$ m/s	$V = 0.8$ m/s	$V = 1.2$ m/s
L_{stable}	3.90	4.00	3.95
$L_{unstable}$	3.60	3.60	3.55

In Figure 13, L_{stable} is marked with a cross for a time delay τ_2, and $L_{unstable}$ with a square. It can be seen that the experimental results presented in this section are also in concordance with the results

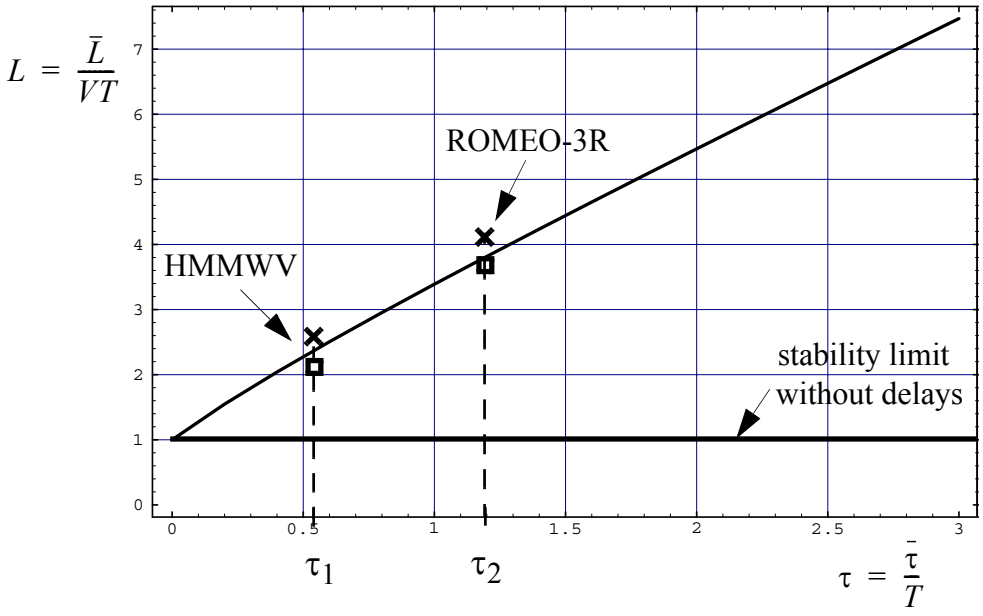

Figure 13: Straight path experimental results.

predicted considering the time delay using the method proposed in this paper.

5.3 Circular path tracking experiments.

These experiments were done with the ROMEO 3R following a circular path of constant curvature ($\gamma^{path} = 0.5$). For circular paths, experiments were done only with velocities of 0.4 and 0.8 m/s, due to the practical difficulties of tracking paths of large curvature at higher velocities. As was done in the straight path experiments, two values were recorded in each test: the minimum stable L (L_{stable}) and the maximum unstable L ($L_{unstable}$). The results are presented in Table 3.

Table 3: ROMEO-3R experimental results

	$V = 0.4$ m/s	$V = 0.8$ m/s
L_{stable}	3.90	4.00
$L_{unstable}$	3.60	3.60

In Figure 14 these values are shown superimposed with the theoretical results obtained in the preceding sections. For clarity, only one of the values is plotted (the worst case): L_{stable} is represented with a cross, and $L_{unstable}$ with a square. The stability limit corresponding to the time delay τ_2 should be between the cross and the square. The theoretical limit value if the time delay is not considered ($L = 1$) is represented with a solid horizontal line.

It can be noted that for circular paths, the non-dimensional stability limit $L = \overline{L}/VT$ has a different value for each velocity, due to the dependence of the non-dimensional path constant curvature of the

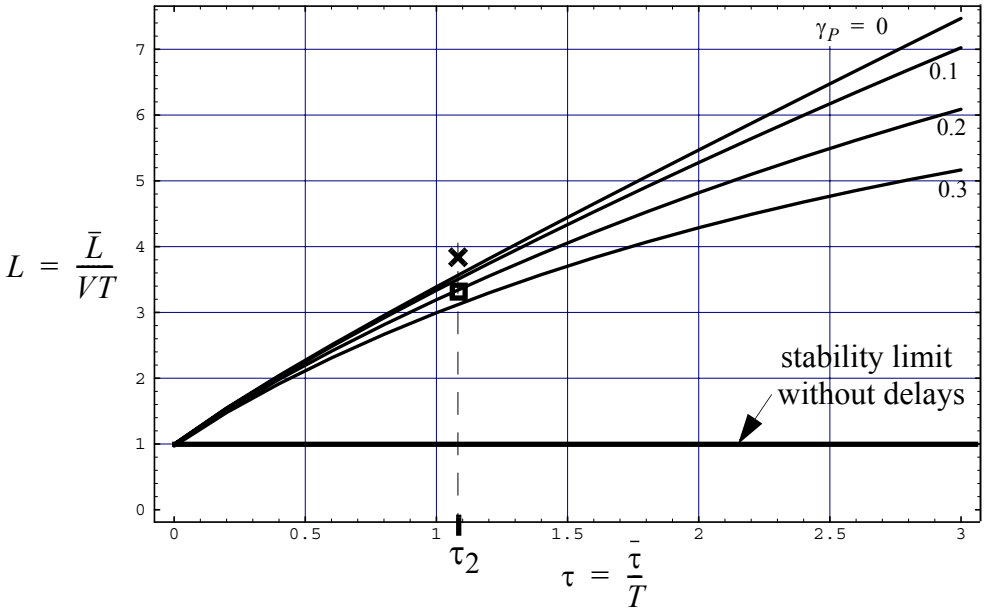

Figure 14: Circular path experimental results.

velocity of the vehicle ($\gamma_p = VT\gamma^{path}$), as can be seen in Figure 9. But in this case, the values were very similar (less than 1% difference). As was the case for straight paths, the experimental results agree with the predictions considering the time delay.

6 Conclusions.

A new approach to analyze the stability of a general class of mobile robot path tracking algorithms taking into account the pure delay in the control loop has been presented. The problem is analyzed solving directly the transcendental characteristic equation, that appears when the time delay is considered. The analysis has been done for straight paths and paths of constant curvature. This has sufficient generality since in most usual operating conditions in autonomous path tracking, the path can be approximated by connected segments of constant curvature. The method has been applied to autonomous path tracking using the pure pursuit algorithm, one of the most widely used, and the results have been checked with simulations. It can be used directly to analyze the stability of any geometric path tracking algorithm. Furthermore the proposed method can be also applied to supervise adaptive systems.

Experimental verification is imperative due to the difficulties to have good models coping with terrain interactions in realistic navigation conditions. This experimental verification is difficult due to the need of performing tests near or over the stability limits. This is dangerous for the expensive autonomous vehicles or even for the people. However, several experiments have been performed with two different autonomous vehicles (ROMEO-3R in the University of Seville, Spain, and a computer controlled HMMWV in Pittsburgh, USA). These tests show good agreement with the theoretical predictions of

the proposed method.

The results presented in this paper can be applied to tune the lookahead distance of the path tracking algorithm for a given path, which is a critical parameter for the performance of the algorithm. It can also be used to obtain the maximum velocity that the vehicle can maintain for a particular path.

7 Acknowledgments.

The work presented in this paper has been partially supported by the Spanish CICYT projects TAP99-0926-C04-01 and DPI2002-04401-C03-03. The authors also gratefully acknowledge assistance from Omead Amidi at the VASC (Robotics Institute, CMU), and Ben Motazed, Jeff Callen and Demetri Patukas from RedZone Robotics, Inc. (Pittsburgh, PA, USA).

REFERENCES

[1] T. Schonberg, M. Ojala, J. Suomela, A. Torpo and A. Halme, Positioning an autonomous off-road vehicle by using fused DGPS and inertial navigation, in *IFAC Conf. on Intelligent Autonomous Vehicles (IAV95)*, Finland, pp.226-231 (1995).

[2] A. Rodriguez-Castaño, G. Heredia and A. Ollero, Fuzzy path tracking and position estimation of autonomous vehicles using differential GPS, *Mathware and Soft Computing*, **2**, 3, pp.257-264 (2000).

[3] D.H. Shin and A. Ollero. Mobile robot path planning for fine-grained and smooth path specifications, *Journal of robotics systems*, **12**, 7, pp.491-503 (1995).

[4] E. Dickmans, B. Mysliwetz and T. Christians, An integrated spatio-temporal approach to automatic visual guidance of autonomous vehicles, *IEEE Trans. on Systems, Man and Cybernetics*, **20**, 6, pp.1273-1284 (1990).

[5] D. Pommerleau, *Neural network perception for mobile robots guidance*, Kluwer Academic (1993).

[6] J. Ferruz and A. Ollero, Integrated real-time vision system for vehicle control in non-structured environments, *Engineering Applications of Artificial Intelligence*, **13**, 3, pp.215-236 (2000).

[7] F. Cuesta and A. Ollero, *Intelligent Mobile Robot Navigation*, Springer (2005).

[8] A. Rodriguez-Castaño, G. Heredia and A. Ollero, Design and implementation of a high-speed autonomous navigation system for heavy vehicles, submitted to *Engineering Applications of Artificial Intelligence* (2006)

[9] D. Shin, *High performance tracking of explicit paths by roadworthy mobile robots*, Ph. D. Dissertation, Carnegie Mellon University (1990).

[10] R. Fenton, G. Melocik and K. Olson, On the steering of automated vehicles: theory and experiment, *IEEE Trans. Automatic Control*, pp.306-315 (1976).

[11] W.H. Cormier and R. Fenton, On the steering of automated vehicles- a velocity-adaptive controller. *IEEE Trans. Automatic Control*, pp.375-385 (1980).

[12] A. Ollero and O. Amidi, Predictive Path Tracking of Mobile Robots-Application to the CMU Navlab, in *Proc. of the Fifth International Conference on Advanced Robotics*, Pisa, Vol. II, pp. 1081-1086 (1991).

[13] C. Canudas de Wit, B. Siciliano, G. Bastin (Eds), *Theory of Robot Control*, Springer, London, UK, ISBN 3540760547 (1996).

[14] C. Samson, Control of chained systems-Application to path following and time-varying point-stabilization of mobile robots, *IEEE Trans. on Automatic Control*, v. 40, pp. 64-77 (1995).

[15] A. Ollero, A. G. Cerezo and J. Martinez, Fuzzy supervisory path tracking of autonomous vehicles, *Control Engineering Practice*, Vol. 2, No. 2, pp. 313-319 (1994).

[16] A. Garcia-Cerezo, A. Ollero and J.L. Martinez, Design of a robust high-performance fuzzy path tracker for autonomous vehicles, *IEEE International Journal of Systems Science*, Vol. 27, No. 8, pp.799-806 (1996).

[17] J. Slotine and W. Li, *Applied Nonlinear Control*, Prentice Hall (1991).

[18] J. Aracil, G. Heredia and A. Ollero, Global stability analisys of fuzzy path tracking using frequency response, *Engineering Applications of Artificial Intelligence*, Vol. 13(2), pp.109-119 (2000).

[19] G. Heredia, A. Ollero, F. Gordillo and J. Aracil, Stability analysis of fuzzy path tracking using a MIMO frequency response technique, in *Proc. of the IFAC Workshop on Intelligent Components for Vehicles (ICV98)*, Sevilla (1998).

[20] G.M. Schoen, *Stability and stabilization of time-delay systems*, Ph. D. Dissertation, ETH Zurich, No. 11166 (1995).

[21] A. Thowsen, An analytic stability test for a class of time-delay systems, *IEEE Trans. on Automatic Control*, Vol. 26, No. 3, pp. 735-736 (1981).

[22] R. Hertz, E. I. Jury and E. Zeheb, Simplified analytical stability test for systems with commensurate time-delays, *IEE Proceedings, Pt. D*, Vol. 131, No. 1, pp. 52-56 (1984).

[23] N. Sarkar, X. Yun and V. Kumar, Control of mechanical systems with rolling constraints: application to dynamic control of mobile robots, *I. J. Robotic Research*, Vol. 13, No 1, pp 55-69 (1994).

[24] O. Amidi, *Integrated mobile robot control*, Carnegie Mellon University, Robotics Institute, Technical Report CMU-RI-TR-90-17 (1990).

[25] H. Gorecki, S. Fuksa, P. Grabowski and A. Korytowski, *Analysis and Synthesis of Time Delay Systems*, John Wiley & Sons, New York (1989).

[26] A. Ollero, B. Arrue, J. Ferruz, G. Heredia, F. Cuesta, F. Lpez-Pichaco and C. Nogales, Control and perception components for autonomous vehicle guidance. Application to the ROMEO vehicles, *Control Engineering Practice*, Vol. 7, pp. 1291-1299 (1999).

[27] A. Ollero and G. Heredia, Stability Analysis of Mobile Robot Path Tracking, in *IEEE/RSJ International Conference on Intelligent Robots and Systems (IROS95)*, Pittsburgh, USA, pp. 461-466 (1995).

Figure 10 a) ROMEO-3R **b) HMMWV from RedZone Robotics**